Journal of Quantitative Spectroscopy & Radiative Transfer 110 (2009) 43–50

Contents lists available at ScienceDirect

Journal of Quantitative Spectroscopy & Radiative Transfer

journal homepage: www.elsevier.com/locate/jqsrt

General derivation of the total electromagnetic cross sections for an arbitrary particle

M.J. Berg, A. Chakrabarti, C.M. Sorensen *

Department of Physics, Kansas State University, Manhattan, KS 66506-2601, USA

ARTICLE INFO

Article history:
Received 24 July 2008
Received in revised form
17 September 2008
Accepted 18 September 2008

Keywords:
Electromagnetic scattering
Light scattering
Extinction cross section
Scattering cross section
Absorption cross section
Vector spherical waves
Vector spherical harmonics
Near field
Far field

ABSTRACT

This work concerns a common problem in electromagnetic scattering; calculation of the total scattering, extinction, and absorption cross sections for an arbitrary particle. Typical expressions for the cross sections are obtained in terms of the vector spherical wave function expansions for the incident and scattered waves. The unique aspect of this work is that the derivation is carried out specifically without use of the far-field zone approximation. The resulting expressions, valid at any distance, exactly match those obtained from the far-field approximation. This demonstrates that the cross sections are independent of the distance from the particle at which they are calculated as one would expect from energy conservation. Numerical simulations of the near and far-field zone energy flows due to a spherical particle are presented to illustrate several implications of this result.

1. Introduction

The total extinction C^{ext}, scattering C^{sca}, and absorption C^{abs} cross sections for a particle residing in a *nonabsorbent* medium are nearly always calculated in the particle's far-field zone. This is done partly because the mathematical form of the scattered fields are substantially simpler in the far-field zone, and because most cross section measurements are performed far enough from the particle that the far-field approximation can be quite good. The essential physical significance of the total cross sections is that they collectively account for the redistribution and conservation of energy in the scattering process. Consequently, since the external medium is nonabsorbent, one would expect that expressions for these cross sections should be independent of the distance from the particle at which they are calculated. The intent of this work is to explicitly demonstrate how exact expressions for the total cross sections can be found that are independent of distance from the particle. This is done by explicitly evaluating integral expressions for the cross sections in a particle's near-field zone. The exact equivalence of the resulting expressions to those that are derived in the far-field zone proves the distance independence. Numerical simulations of spherical particles are presented that verify the equivalence of the cross sections when calculated in the near and far-field zones and help illustrate the physical significance of this result.

It should be noted that this work is not the first to calculate a particle's cross sections in the near-field. For example, work by Grandy and Bohren and Huffman mentions that C^{sca} and C^{abs} can be calculated for a spherical particle using a surface, like S_{en} described below, that is of arbitrary size but does not show the details of the calculation [1,2]. Videen et al.

* Corresponding author.
E-mail address: sor@phys.ksu.edu (C.M. Sorensen).

0022-4073/$ - see front matter © 2008 Elsevier Ltd. All rights reserved.
doi:10.1016/j.jqsrt.2008.09.008

and Fu et al. find near-field expressions for the cross sections for a particle embedded in an *absorbing* medium [3,4]. Further relevant work related to particles in an absorbing medium can be found in [5] and references therein. To the authors' knowledge, the following calculations are the first to consider an *arbitrary* particle and formulate and evaluate exact expressions for the total cross sections valid at *any* distance.

2. Derivation of the cross sections

Consider a fixed arbitrarily shaped particle residing in vacuum and illuminated by a linearly polarized incident plane wave. The particle's complex-valued refractive index m is also arbitrary. The particle is centered at the coordinate origin $\mathcal{O}$ and its surface, internal volume, and external region are denoted by S, V^{int} and V^{ext}, respectively, see Fig. 1. Surrounding the particle is its smallest circumscribing sphere S_{sc} of radius R_{sc}. The purpose of this sphere is to define the minimum distance from the origin beyond which one is guaranteed that the vector spherical wave function (VSWF) expansions of Eqs. (5), (6), (8), and (9) below will converge, see [6]. Also enclosing the particle, and S_{sc}, is another spherical surface S_{en} of radius R_{en}. This sphere will be used as the closed surface over which the fields will be integrated in Eqs. (11) and (12) to yield expressions for the total cross sections.

The wave incident on the particle is a linearly polarized plane wave traveling along the $\hat{\mathbf{n}}^{\text{inc}}$ direction with a wavenumber $k = 2\pi/\lambda$, where λ is the vacuum wavelength. The time dependence of the wave is harmonic and given by $\exp(-\mathrm{i}\omega t)$ where ω is the angular frequency, $\omega = kc$, and c is the speed of light in vacuum. The time dependence will be suppressed in the following for brevity. The electric and magnetic fields of this incident wave are

$$\mathbf{E}^{\text{inc}}(\mathbf{r}) = \mathbf{E}_0^{\text{inc}} \exp(\mathrm{i}kr\hat{\mathbf{n}}^{\text{inc}} \cdot \hat{\mathbf{r}}), \tag{1}$$

$$\mathbf{B}^{\text{inc}}(\mathbf{r}) = \frac{k}{\omega}\hat{\mathbf{n}}^{\text{inc}} \times \mathbf{E}^{\text{inc}}(\mathbf{r}), \tag{2}$$

respectively, where $\mathbf{E}_0^{\text{inc}}$ is a constant vector describing the amplitude and polarization of the wave.

The presence of the particle in the incident wave establishes a new (total) wave that can be *mathematically* regarded as the superposition of the incident and scattered waves. The total electric and magnetic fields outside of the particle are then

$$\mathbf{E}(\mathbf{r}) = \mathbf{E}^{\text{inc}}(\mathbf{r}) + \mathbf{E}^{\text{sca}}(\mathbf{r}), \tag{3}$$

$$\mathbf{B}(\mathbf{r}) = \mathbf{B}^{\text{inc}}(\mathbf{r}) + \mathbf{B}^{\text{sca}}(\mathbf{r}). \tag{4}$$

These fields can be expanded into series of VSWFs as

$$\mathbf{E}^{\text{inc}}(\mathbf{r}) = \sum_{n=1}^{\infty}\sum_{m=-n}^{n}[a_{mn}\,\text{Rg}\,\mathbf{M}_{mn}(k\mathbf{r}) + b_{mn}\,\text{Rg}\,\mathbf{N}_{mn}(k\mathbf{r})], \quad \mathbf{r} \in V^{\text{int}} \cup V^{\text{ext}}, \tag{5}$$

$$\mathbf{E}^{\text{sca}}(\mathbf{r}) = \sum_{n=1}^{\infty}\sum_{m=-n}^{n}[p_{mn}\mathbf{M}_{mn}(k\mathbf{r}) + q_{mn}\mathbf{N}_{mn}(k\mathbf{r})], \quad \mathbf{r} \in V^{\text{ext}}. \tag{6}$$

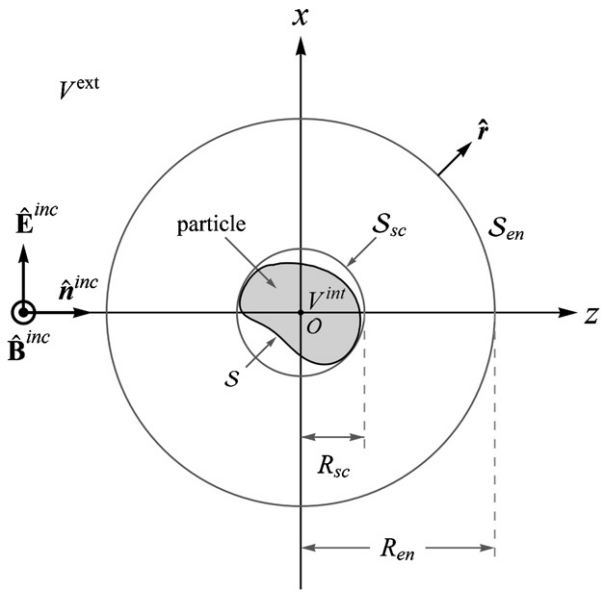

Fig. 1. Scattering arrangement showing an arbitrary particle illuminated by a linearly polarized incident plane wave.

The properties of the VSWFs **M**, **N**, Rg**M**, and Rg**N** in Eqs. (5) and (6) needed in the following calculations are given in Appendix A. A more complete collection of VSWF properties and their definitions is given in [6, Appendix C]. The VSWFs constitute a complete set of orthogonal functions satisfying the free-space vector Helmholtz wave equation, making them a convenient set to expand the fields external to the particle [6,7]. The functions **M** and **N** obey the Sommerfeld radiation condition at $kr \to \infty$ but diverge at the origin. Thus, these functions are suited for expansion of the scattered field while concomitantly restricting the observation point **r** to reside outside of S_{sc}, i.e. $\mathbf{r} \in V^{ext}$. The functions Rg**M**, and Rg**N** are the regular VSWFs, which are finite at the origin and hence suited for expansion of the incident field.

Using the Maxwell curl equation

$$\nabla \times \mathbf{E}(\mathbf{r}) = \mathrm{i}\omega \mathbf{B}(\mathbf{r}), \tag{7}$$

along with Eqs. (36)–(38) in Appendix A, one can derive expressions for the incident and scattered magnetic fields from Eqs. (5) and (6) as

$$\mathbf{B}^{inc}(\mathbf{r}) = \frac{-\mathrm{i}k}{\omega} \sum_{n=1}^{\infty} \sum_{m=-n}^{n} [a_{mn}\, \mathrm{Rg}\,\mathbf{N}_{mn}(k\mathbf{r}) + b_{mn}\, \mathrm{Rg}\,\mathbf{M}_{mn}(k\mathbf{r})], \quad \mathbf{r} \in V^{int} \cup V^{ext}, \tag{8}$$

$$\mathbf{B}^{sca}(\mathbf{r}) = \frac{-\mathrm{i}k}{\omega} \sum_{n=1}^{\infty} \sum_{m=-n}^{n} [p_{mn}\mathbf{N}_{mn}(k\mathbf{r}) + q_{mn}\mathbf{M}_{mn}(k\mathbf{r})], \quad \mathbf{r} \in V^{ext}. \tag{9}$$

Expressions for the total cross sections are obtained by integrating the component of the total flow of electromagnetic energy passing through a closed surface enclosing the particle, see [6, Section 2.8]. The spherical surface S_{en} will serve as this closed surface and the flow of electromagnetic energy is given by the time-averaged Poynting vector $\langle \mathbf{S} \rangle_t$ [8],

$$\langle \mathbf{S}(\mathbf{r}) \rangle_t = \frac{1}{2\mu_0} \mathrm{Re}\{\mathbf{E}(\mathbf{r}) \times [\mathbf{B}(\mathbf{r})]^*\}. \tag{10}$$

In Eq. (10), the asterisk denotes complex conjugation, $\langle \ldots \rangle_t$ denotes time averaging, and Re{…} is the real filter. Using Eqs. (3), (4), and (10) and noting that the radial unit vector $\hat{\mathbf{r}}$ is also the outward surface normal for S_{en}, one can obtain the following expressions for the total extinction and scattering cross sections in terms of the fields explicitly:

$$C^{ext} = -\frac{1}{2\mu_0 I^{inc}} \mathrm{Re} \oint_{S_{en}} \{\mathbf{E}^{inc}(\mathbf{r}) \times [\mathbf{B}^{sca}(\mathbf{r})]^* + \mathbf{E}^{sca}(\mathbf{r}) \times [\mathbf{B}^{inc}(\mathbf{r})]^*\} \cdot \hat{\mathbf{r}}\, \mathrm{d}S, \tag{11}$$

$$C^{sca} = \frac{1}{2\mu_0 I^{inc}} \mathrm{Re} \oint_{S_{en}} \{\mathbf{E}^{sca}(\mathbf{r}) \times [\mathbf{B}^{sca}(\mathbf{r})]^*\} \cdot \hat{\mathbf{r}}\, \mathrm{d}S, \tag{12}$$

where $I^{inc} = (1/2)\sqrt{\varepsilon_0/\mu_0}|\mathbf{E}_0^{inc}|^2$ is the intensity of the incident wave. See [6,9,10] for more detail concerning the derivation and physical meaning of Eqs. (11) and (12).

The size of S_{en} in Eqs. (11) and (12), given by R_{en}, is arbitrary provided that $R_{en} \geqslant R_{sc}$. Consequently, one usually regards R_{en} as being large enough that S_{en} resides in the particle's far-field zone. This permits approximation of the scattered fields of Eqs. (3) and (4) as outward-traveling transverse spherical waves and justifies use of the optical theorem; this significantly simplifies the evaluation of Eqs. (11) and (12), see [11,12].

In the following sections, the VSWF expansions of Eqs. (5), (6), (8), and (9) are combined with Eqs. (11) and (12) to arrive at general expressions for C^{ext} and C^{sca}. This is done specifically *without* any assumption regarding the size of S_{en} and *without* invoking the far-field approximation. One will see that the calculation of C^{ext} and C^{sca}, while somewhat more mathematically involved, yields expressions for the cross sections that are *exactly* identical to those that would result from use of the far-field approximation.

2.1. The extinction cross section

Combining Eqs. (5), (6), (8), and (9) with Eq. (11), grouping terms with common expansion coefficients and using the vector identity $(\mathbf{b} \times \mathbf{c}) \cdot \mathbf{a} = \mathbf{c} \cdot (\mathbf{a} \times \mathbf{b})$ gives

$$\begin{aligned} C^{ext} = & -c_0\, \mathrm{Re} \oint_{S_{en}} \mathrm{i} \sum_{n=1}^{\infty} \sum_{m=-n}^{n} \sum_{n'=1}^{\infty} \sum_{m'=-n'}^{n'} \{a_{m'n'}(p_{mn})^* \mathbf{N}_{mn}^*(k\mathbf{r}) \cdot [\hat{\mathbf{r}} \times \mathrm{Rg}\mathbf{M}_{m'n'}(k\mathbf{r})] \\ & + (a_{m'n'})^* p_{mn}\, \mathrm{Rg}\,\mathbf{N}_{m'n'}^*(k\mathbf{r}) \cdot [\hat{\mathbf{r}} \times \mathbf{M}_{mn}(k\mathbf{r})] + b_{m'n'}(q_{mn})^* \mathbf{M}_{mn}^*(k\mathbf{r}) \cdot [\hat{\mathbf{r}} \times \mathrm{Rg}\,\mathbf{N}_{m'n'}(k\mathbf{r})] \\ & + (b_{m'n'})^* p_{mn}\, \mathrm{Rg}\,\mathbf{M}_{m'n'}^*(k\mathbf{r}) \cdot [\hat{\mathbf{r}} \times \mathbf{N}_{mn}(k\mathbf{r})] + b_{m'n'}(p_{mn})^* \mathbf{N}_{mn}^*(k\mathbf{r}) \cdot [\hat{\mathbf{r}} \times \mathrm{Rg}\,\mathbf{N}_{m'n'}(k\mathbf{r})] \\ & + (a_{m'n'})^* q_{mn}\, \mathrm{Rg}\,\mathbf{N}_{m'n'}^*(k\mathbf{r}) \cdot [\hat{\mathbf{r}} \times \mathbf{N}_{mn}(k\mathbf{r})] + a_{m'n'}(q_{mn})^* \mathbf{M}_{mn}^*(k\mathbf{r}) \cdot [\hat{\mathbf{r}} \times \mathrm{Rg}\,\mathbf{M}_{m'n'}(k\mathbf{r})] \\ & + (b_{m'n'})^* p_{mn}\, \mathrm{Rg}\,\mathbf{M}_{m'n'}^*(k\mathbf{r}) \cdot [\hat{\mathbf{r}} \times \mathbf{M}_{mn}(k\mathbf{r})]\}\, \mathrm{d}S, \end{aligned} \tag{13}$$

where $c_0 = k/2\omega\mu_0 I^{inc}$. Next, using appendix Eqs. (40)–(48) show that the following terms in Eq. (13) become

$$\oint_{S_{en}} \mathbf{M}_{mn}^*(k\mathbf{r}) \cdot [\hat{\mathbf{r}} \times \mathrm{Rg}\,\mathbf{M}_{m'n'}(k\mathbf{r})]\, \mathrm{d}S = 0, \tag{14}$$

$$\oint_{S_{\mathrm{en}}} \mathrm{Rg}\,\mathbf{M}^*_{m'n'}(k\mathbf{r})\cdot[\hat{\mathbf{r}}\times\mathbf{M}_{mn}(k\mathbf{r})]\,\mathrm{d}S=0, \tag{15}$$

$$\oint_{S_{\mathrm{en}}} \mathbf{N}^*_{mn}(k\mathbf{r})\cdot[\hat{\mathbf{r}}\times\mathrm{Rg}\,\mathbf{N}_{m'n'}(k\mathbf{r})]\,\mathrm{d}S=0, \tag{16}$$

$$\oint_{S_{\mathrm{en}}} \mathrm{Rg}\,\mathbf{N}^*_{m'n'}(k\mathbf{r})\cdot[\hat{\mathbf{r}}\times\mathbf{N}_{mn}(k\mathbf{r})]\,\mathrm{d}S=0. \tag{17}$$

Using the orthogonality relation of Eq. (49) along with Eqs. (40)–(44) on the remaining terms in Eq. (13) eventually gives

$$\begin{aligned}C^{\mathrm{ext}} = &-c_0R_{\mathrm{en}}^2\,\mathrm{Re}\sum_{n=1}^{\infty}\sum_{m=-n}^{n}\Big\{\mathrm{i}a_{mn}(p_{mn})^*\frac{1}{kR_{\mathrm{en}}}[kR_{\mathrm{en}}[h_n^{(1)}(kR_{\mathrm{en}})]^*]'j_n(kR_{\mathrm{en}})+\mathrm{i}(a_{mn})^*p_{mn}\frac{1}{kR_{\mathrm{en}}}[kR_{\mathrm{en}}j_n(kR_{\mathrm{en}})]'h_n^{(1)}(kR_{\mathrm{en}})\\&-\mathrm{i}b_{mn}(q_{mn})^*\frac{1}{kR_{\mathrm{en}}}[kR_{\mathrm{en}}j_n(kR_{\mathrm{en}})]'[h_n^{(1)}(kR_{\mathrm{en}})]^*-\mathrm{i}(b_{mn})^*q_{mn}\frac{1}{kR_{\mathrm{en}}}[kR_{\mathrm{en}}h_n^{(1)}(kR_{\mathrm{en}})]'j_n(kR_{\mathrm{en}})\Big\},\end{aligned} \tag{18}$$

where $[kR_{\mathrm{en}}h_n^{(1)}(kR_{\mathrm{en}})]'$ denotes differentiation with respect to kR_{en}. This expression is simplified using the linear independence of the spherical Bessel and Hankel functions via the Wronskian relation [13]

$$W_1=[kR_{\mathrm{en}}j_n(kR_{\mathrm{en}})]'h_n^{(1)}(kR_{\mathrm{en}})-[kR_{\mathrm{en}}h_n^{(1)}(kR_{\mathrm{en}})]'j_n(kR_{\mathrm{en}})=-\frac{\mathrm{i}}{kR_{\mathrm{en}}}. \tag{19}$$

With Eq. (19), and keeping in mind that the spherical Bessel functions of the first kind j_n are real-valued since their argument is real-valued, Eq. (18) can be reduced to

$$C^{\mathrm{ext}}=-\frac{1}{k^2|\mathbf{E}_0^{\mathrm{inc}}|^2}\sum_{n=1}^{\infty}\sum_{m=-n}^{n}\mathrm{Re}[a_{mn}(p_{mn})^*+b_{mn}(q_{mn})^*]. \tag{20}$$

One can verify that Eq. (20) is exactly the same expression for C^{ext} obtained from use of the far-field approximation for the scattered wave in combination with the optical theorem, e.g. see [6, Eq. (5.18a); 7, pp. 60–61].

2.2. The scattering cross section

Combining Eqs. (6) and (9) with (12) and using the vector identity $(\mathbf{b}\times\mathbf{c})\cdot\mathbf{a}=\mathbf{c}\cdot(\mathbf{a}\times\mathbf{b})$ gives for the scattering cross section

$$\begin{aligned}C^{\mathrm{sca}} = c_0\,\mathrm{Re}\oint_{S_{\mathrm{en}}}\mathrm{i}\sum_{n=1}^{\infty}\sum_{m=-n}^{n}\sum_{n'=1}^{\infty}\sum_{m'=-n'}^{n'}&\{p_{mn}(p_{m'n'})^*\mathbf{N}^*_{m'n'}(k\mathbf{r})\cdot[\hat{\mathbf{r}}\times\mathbf{M}_{mn}(k\mathbf{r})]+p_{mn}(q_{m'n'})^*\mathbf{M}^*_{m'n'}(k\mathbf{r})\cdot[\hat{\mathbf{r}}\times\mathbf{M}_{mn}(k\mathbf{r})]\\&+(p_{m'n'})^*q_{mn}\mathbf{N}^*_{m'n'}(k\mathbf{r})\cdot[\hat{\mathbf{r}}\times\mathbf{N}_{mn}(k\mathbf{r})]+q_{mn}(q_{m'n'})^*\mathbf{M}^*_{m'n'}(k\mathbf{r})\cdot[\hat{\mathbf{r}}\times\mathbf{N}_{mn}(k\mathbf{r})]\}\,\mathrm{d}S.\end{aligned} \tag{21}$$

From appendix Eqs. (40), (42) and (44)–(48), one finds that

$$\oint_{S_{\mathrm{en}}} \mathbf{M}^*_{m'n'}(k\mathbf{r})\cdot[\hat{\mathbf{r}}\times\mathbf{M}_{mn}(k\mathbf{r})]\,\mathrm{d}S=0, \tag{22}$$

$$\oint_{S_{\mathrm{en}}} \mathbf{N}^*_{m'n'}(k\mathbf{r})\cdot[\hat{\mathbf{r}}\times\mathbf{N}_{mn}(k\mathbf{r})]\,\mathrm{d}S=0, \tag{23}$$

which reduces Eq. (21) to

$$C^{\mathrm{sca}}=\frac{c_0R_{\mathrm{en}}}{k}\sum_{n=1}^{\infty}\sum_{m=-n}^{n}\mathrm{Re}\{\mathrm{i}|p_{mn}|^2[kR_{\mathrm{en}}[h_n^{(1)}(kR_{\mathrm{en}})]^*]'h_n^{(1)}(kR_{\mathrm{en}})-\mathrm{i}|q_{mn}|^2[kR_{\mathrm{en}}h_n^{(1)}(kR_{\mathrm{en}})]'[h_n^{(1)}(kR_{\mathrm{en}})]^*\}. \tag{24}$$

To simplify Eq. (24), first recall that $h_n^{(1)}$ and $h_n^{(2)}$ are related to j_n and y_n as

$$h_n^{(1)}(kr)=j_n(kr)+\mathrm{i}y_n(kr), \tag{25}$$

$$h_n^{(2)}(kr)=j_n(kr)-\mathrm{i}y_n(kr). \tag{26}$$

The argument of the spherical Bessel functions j_n and y_n is real-valued outside of the particle since the external medium is nonabsorbent. Consequently, the functions are also real-valued. Then, Eqs. (25) and (26) show that

$$h_n^{(2)}(kR_{\mathrm{en}})=[h_n^{(1)}(kR_{\mathrm{en}})]^*. \tag{27}$$

Using Eq. (27) with Eq. (24) gives

$$C^{\mathrm{sca}}=\frac{c_0R_{\mathrm{en}}}{k}\sum_{n=1}^{\infty}\sum_{m=-n}^{n}[|p_{mn}|^2\,\mathrm{Re}\{\mathrm{i}[kR_{\mathrm{en}}h_n^{(2)}(kR_{\mathrm{en}})]'h_n^{(1)}(kR_{\mathrm{en}})\}-|q_{mn}|^2\,\mathrm{Re}\{\mathrm{i}[kR_{\mathrm{en}}h_n^{(1)}(kR_{\mathrm{en}})]'h_n^{(2)}(kR_{\mathrm{en}})\}]. \tag{28}$$

The Wronskian relation for the spherical Bessel functions of the first and second kind is [14]

$$W_2 = j_n(kR_{\rm en})y_n'(kR_{\rm en}) - y_n(kR_{\rm en})j_n'(kR_{\rm en}) = \frac{1}{(kR_{\rm en})^2}. \tag{29}$$

By using Eq. (29) and by neglecting all terms that are pure imaginary due to the presence of the Re{...} filter, one eventually finds that the first term in Eq. (28) is

$$\mathrm{Re}\{\mathrm{i}[kR_{\rm en}h_n^{(2)}(kR_{\rm en})]'h_n^{(1)}(kR_{\rm en})\} = \frac{1}{kR_{\rm en}}, \tag{30}$$

and that the second term is

$$\mathrm{Re}\{-\mathrm{i}[kR_{\rm en}h_n^{(1)}(kR_{\rm en})]'h_n^{(2)}(kR_{\rm en})\} = -\frac{1}{kR_{\rm en}}. \tag{31}$$

With Eqs. (30) and (31), the total scattering cross section of Eq. (28) becomes

$$C^{\rm sca} = \frac{1}{k^2|\mathbf{E}_0^{\rm inc}|^2}\sum_{n=1}^{\infty}\sum_{m=-n}^{n}\{|p_{mn}|^2 + |q_{mn}|^2\}, \tag{32}$$

which is exactly what one would expect from use of the far-field approximation for the scattered wave, e.g. see [6, Eq. (5.18b)].

2.3. The absorption cross section

From energy conservation considerations, one finds that the extinction, scattering, and absorption cross sections are related by

$$C^{\rm ext} = C^{\rm sca} + C^{\rm abs}, \tag{33}$$

see for example [9,10]. With this relationship, Eqs. (20) and (32) can be combined to yield the total absorption cross section,

$$C^{\rm abs} = -\frac{1}{k^2|\mathbf{E}_0^{\rm inc}|^2}\sum_{n=1}^{\infty}\sum_{m=-n}^{n}\{\mathrm{Re}[a_{mn}(p_{mn})^* + b_{mn}(q_{mn})^*] + |p_{mn}|^2 + |q_{mn}|^2\}. \tag{34}$$

3. Numerical examples

Eqs. (20), (32), and (34) are *exact* expressions. No approximations, specifically the far-field approximation, are needed for their derivation. The expressions are valid for a particle of any shape and composition provided that it resides in a nonabsorbent medium and is illuminated by a linearly polarized electromagnetic plane wave. In what follows numerical examples involving spherical particles will be presented that demonstrate implications of the above results.

Consider the calculation of $C^{\rm sca}$ for a spherical particle with $kR = 50$ and $m = 1.10 + 0\mathrm{i}$. The scattering cross section is determined by the term in the total energy flow of Eq. (10) involving only the fields of the scattered wave,

$$\langle \mathbf{S}^{\rm sca}(\mathbf{r})\rangle_t = \frac{1}{2\mu_0}\,\mathrm{Re}\{\mathbf{E}^{\rm sca}(\mathbf{r}) \times [\mathbf{B}^{\rm sca}(\mathbf{r})]^*\}, \tag{35}$$

see [6, Section 2.8]. To calculate $C^{\rm sca}$ from Eq. (35), the radial component of the energy flow is integrated over $S_{\rm en}$. Recall that the radius of this surface $R_{\rm en}$ is arbitrary; $S_{\rm en}$ can be either in the particle's near or far-field zone.

Fig. 2 shows the energy flow of Eq. (35) for the spherical particle in the near and far-field zones, plots (a) and (b), respectively. In plot (a), the energy flow that is shown on the inside of the particle is the total flow of Eq. (10) given by the internal fields. In plot (b), the energy flow is multiplied by r^2 to reveal its angular structure. The incident wave propagates along the z-axis from left to right and is polarized along the x-axis. All field quantities are calculated from the Mie solution to the Maxwell equations following [2].

One can see that the plots in Fig. 2 show vastly different behavior for the energy flow between the two zones. This difference is no surprise. The scattered wave in the near-field zone can be complicated in form; it can have a longitudinal component and nonspherical surfaces of constant phase and amplitude. In the far-field zone, however, the scattered wave becomes a transverse spherical wave with spherical surfaces of constant phase and amplitude [12]. This gives the far-field energy flow its simple radial-direction and angular magnitude-dependence. Despite the dramatic differences apparent in Fig. 2, the exact same cross sections are obtained from the energy flows.

To numerically demonstrate the distance independence of the cross sections, the extinction efficiency $Q^{\rm ext}$ for several spherical particles is calculated in both the near and far-field zones and presented in Table 1. To do this, the integral in Eq. (11) is numerically evaluated over $S_{\rm en}$ when $R_{\rm en} = 1.001R$. Provided that $kR \gg 1$, as it is in Table 1, this size of $S_{\rm en}$ places the surface in the particle's extreme near-field zone. The resulting value for the cross section will be denoted the near-field extinction cross section $C_{\rm near}^{\rm ext}$. From $C_{\rm near}^{\rm ext}$, the near-field extinction efficiency follows as $Q_{\rm near}^{\rm ext} = C_{\rm near}^{\rm ext}/\pi R^2$.

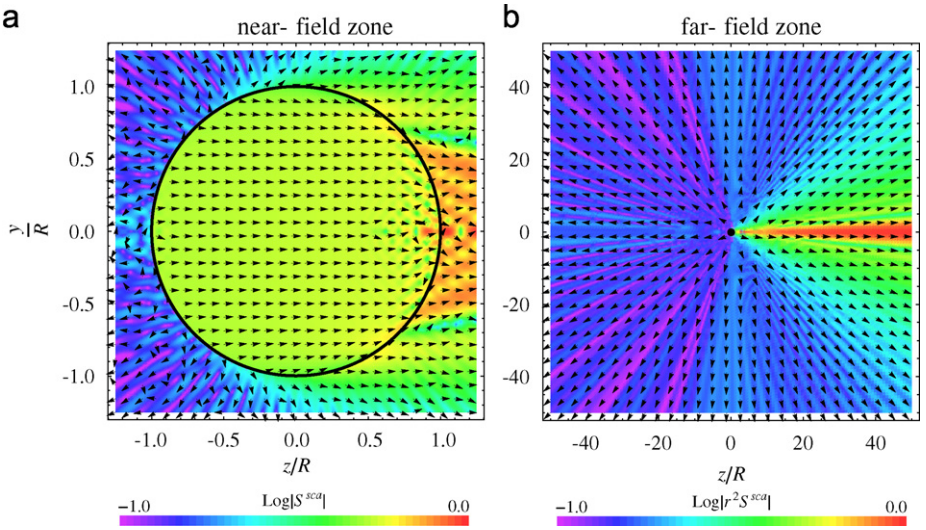

Fig. 2. Time-averaged energy flow due to the scattered wave of a spherical particle with $kR = 50$ and $m = 1.10 + 0\mathrm{i}$. The incident wave travels along the z-axis from left to right and is polarized along the x-axis, normal to the page. Plot (a) shows the energy flow $\langle \mathbf{S}^{\mathrm{sca}} \rangle_t$ of Eq. (35) in the sphere's near field zone outside the particle, and the total energy flow of Eq. (10) inside the particle. Plot (b) shows $r^2 \langle \mathbf{S}^{\mathrm{sca}} \rangle_t$ in the particle's far-field zone; the flow is multiplied by r^2 to help reveal its angular structure. Both plots show the y–z plane through the origin, which slices the sphere along its equator. The color shades indicate the magnitude of the energy flow in log scale with the largest magnitude normalized to unity, i.e. $\log(1.0) = 0.0$.

Table 1
Values of the extinction efficiency factor for spherical particles calculated in the near and far-field zones

kR	m	$Q^{\mathrm{ext}}_{\mathrm{near}}$	$Q^{\mathrm{ext}}_{\mathrm{far}}$
50.00	$1.100 + 0.000\mathrm{i}$	2.449	2.446
50.00	$1.330 + 1.000 \times 10^{-6}\mathrm{i}$	1.980	1.982
25.00	$1.750 + 0.440\mathrm{i}$	2.224	2.221
25.00	$1.010 + 1.000\mathrm{i}$	2.233	2.231
10.00	$10.00 + 0.000\mathrm{i}$	2.106	2.104

For comparison, the extinction cross section in the particle's far-field zone, denoted $C^{\mathrm{ext}}_{\mathrm{far}}$, is calculated using the optical theorem, e.g. see [6, p. 57]. This gives a far-field extinction efficiency $Q^{\mathrm{ext}}_{\mathrm{far}} = C^{\mathrm{ext}}_{\mathrm{far}}/\pi R^2$.

Table 1 shows values for $Q^{\mathrm{ext}}_{\mathrm{near}}$ and $Q^{\mathrm{ext}}_{\mathrm{far}}$ for spherical particles of vastly different size kR and refractive index m. One can see that the efficiency factors are equivalent to 0.1%. The disagreement between $Q^{\mathrm{ext}}_{\mathrm{near}}$ and $Q^{\mathrm{ext}}_{\mathrm{far}}$ is due to the discretization of the surface integral in Eq. (11) that is required to evaluate $Q^{\mathrm{ext}}_{\mathrm{near}}$ numerically.

4. Comments

As mentioned in Section 1, one typically calculates a particle's total cross section using the far-field zone approximation for the scattered wave. For example, in the case of the extinction cross section, a far-field scattering amplitude is found that is independent of distance from the particle. Then the optical theorem is used to relate the extinction cross section to the value of the scattering amplitude evaluated in the exact forward direction. The result is an exact expression matching Eq. (20), despite the use of an approximate form for the scattered wave. One might then wonder how an approximation for the scattered wave, i.e. the far-field approximation, can result in an exact expression for the cross section. In using the optical theorem, one tacitly assumes the limit $kR_{\mathrm{en}} \to \infty$, e.g. see [6, Appendix A] and [9,10]. In this *limit*, the far-field zone approximation becomes exact and hence is capable of producing an exact expression for C^{ext}. The point here is that the ability to find exact expressions for the total cross sections using the far-field approximation does not necessarily restrict the validity of the resulting expressions to only the far-field zone.

Another integral quantity that is often of interest is the asymmetry parameter g. This quantity describes the overall tendency for a particle to scatter into the forward or backward directions, see [6, p. 60]. Like the total cross sections, the asymmetry parameter is typically calculated in a particle's far-field zone owing to the mathematical convenience of the far-field approximation. However, since g is ultimately derived from the same field quantities that yield C^{sca}, i.e., the scattered fields, it should be possible to carry out a calculation for g similar to that for C^{sca} above that yields g

for any distance from the particle. Work by Videen et al. shows how this can be done in the context of the same VSWF formalism used above [15].

Notice that if the particle were to reside in an absorbing medium, the total cross sections *would* depend on the distance at which they are calculated, e.g. see [3]. In the context of the calculations in Section 2, an absorbing external medium would make the wavenumber k complex valued. Consequently, the spherical Bessel functions would also become complex valued and one would not be able to use the $\mathrm{Re}\{\ldots\}$ filter in combination with the Wronskians of Eqs. (19) and (29) to remove the R_{en} dependence from Eqs. (18) and (28).

The results of this work are not solely of mathematical interest. In hindsight, one could expect that there must be distance independence to the total cross sections since, collectively, the cross sections are a statement of energy conservation, and as such, they cannot rely on some assumed (far field) distance from the particle. One can extend this mindset to other phenomena in electromagnetic theory. For example, it is known that the extinction cross section for a large particle approaches a value of $C^{\mathrm{ext}} \to 2G$ as the particle's size becomes large compared to the vacuum wavelength, e.g. see [6, pp. 239–241]. Here G is the particle's geometric projection into the forward direction, and this result is known as the extinction paradox. The popular explanations for this paradox are implicitly restricted to the far-field zone only, e.g. [16,17]. The essence of the results above demonstrate that explanations of phenomena like the extinction paradox must be able to apply at all distances from the particle, not just in the far-field zone.

5. Conclusion

This work explicitly shows that the total extinction, scattering, and absorption cross sections for an arbitrary particle are completely independent of the distance from the particle at which they are calculated. This expected result is derived within the exact and analytic framework of the vector spherical wave function expansions for the particle's incident and scattered fields. An example of the near and far-field energy flows corresponding to a spherical particle is presented that illustrates the dramatically different form that the flows have in the two zones; this accentuates the remarkable fact that either zone's flow yields exactly the same total cross sections.

Acknowledgments

The authors are thankful for comments provided by O. Larry Weaver, Gorden Videen, and Michael Mishchenko.

Appendix A. Selected properties of the vector spherical wave functions

The following properties of the VSWFs and the vector spherical harmonics (VSHs) can be found in [6, Appendix C] but are repeated here for completeness.

The curl relationships between the VSWF and the regular VSWF are

$$\mathbf{M}_{mn}(k\mathbf{r}) = \frac{1}{k}\nabla \times \mathbf{N}_{mn}(k\mathbf{r}), \tag{36}$$

$$\mathbf{N}_{mn}(k\mathbf{r}) = \frac{1}{k}\nabla \times \mathbf{M}_{mn}(k\mathbf{r}), \tag{37}$$

$$\mathrm{Rg}\,\mathbf{M}_{mn}(k\mathbf{r}) = \frac{1}{k}\nabla \times \mathrm{Rg}\,\mathbf{N}_{mn}(k\mathbf{r}), \tag{38}$$

$$\mathrm{Rg}\,\mathbf{N}_{mn}(k\mathbf{r}) = \frac{1}{k}\nabla \times \mathrm{Rg}\,\mathbf{M}_{mn}(k\mathbf{r}). \tag{39}$$

The VSWFs can be expressed in terms of products of the spherical Bessel and Hankel functions of the first kind j_n and $h_n^{(1)}$, respectively, and the VSHs, $\mathbf{B}$, $\mathbf{C}$, and $\mathbf{P}$ as

$$\mathbf{M}_{mn}(k\mathbf{r}) = \gamma_{mn} h_n^{(1)}(kr)\mathbf{C}_{mn}(\hat{\mathbf{r}}), \tag{40}$$

$$\mathrm{Rg}\,\mathbf{M}_{mn}(k\mathbf{r}) = \gamma_{mn} j_n(kr)\mathbf{C}_{mn}(\hat{\mathbf{r}}), \tag{41}$$

$$\mathbf{N}_{mn}(k\mathbf{r}) = \gamma_{mn}\left\{\frac{n(n+1)}{kr} h_n^{(1)}(kr)\mathbf{P}_{mn}(\hat{\mathbf{r}}) + \frac{1}{kr}[kr\, h_n^{(1)}(kr)]'\mathbf{B}_{mn}(\hat{\mathbf{r}})\right\}, \tag{42}$$

$$\mathrm{Rg}\,\mathbf{N}_{mn}(k\mathbf{r}) = \gamma_{mn}\left\{\frac{n(n+1)}{kr} j_n(kr)\mathbf{P}_{mn}(\hat{\mathbf{r}}) + \frac{1}{kr}[kr\, j_n(kr)]'\mathbf{B}_{mn}(\hat{\mathbf{r}})\right\}, \tag{43}$$

where

$$\gamma_{mn} = \sqrt{\frac{(2n+1)(n-m)!}{4\pi n(n+1)(n+m)!}}. \tag{44}$$

The VSHs are interrelated as

$$\mathbf{B}_{mn}(\hat{\mathbf{r}}) = \hat{\mathbf{r}} \times \mathbf{C}_{mn}(\hat{\mathbf{r}}), \tag{45}$$

$$\mathbf{C}_{mn}(\hat{\mathbf{r}}) = -\hat{\mathbf{r}} \times \mathbf{B}_{mn}(\hat{\mathbf{r}}) \tag{46}$$

with the additional property

$$\hat{\mathbf{r}} \times \mathbf{P}_{mn}(\hat{\mathbf{r}}) = 0. \tag{47}$$

The orthogonality relationships for the VSHs are

$$\int_{4\pi} \mathbf{B}_{mn}(\hat{\mathbf{r}}) \cdot \mathbf{C}^*_{m'n'}(\hat{\mathbf{r}})\, \mathrm{d}\Omega = \int_{4\pi} \mathbf{B}^*_{mn}(\hat{\mathbf{r}}) \cdot \mathbf{C}_{m'n'}(\hat{\mathbf{r}})\, \mathrm{d}\Omega = 0, \tag{48}$$

$$\int_{4\pi} \mathbf{B}_{mn}(\hat{\mathbf{r}}) \cdot \mathbf{B}^*_{m'n'}(\hat{\mathbf{r}})\, \mathrm{d}\Omega = \int_{4\pi} \mathbf{C}^*_{mn}(\hat{\mathbf{r}}) \cdot \mathbf{C}_{m'n'}(\hat{\mathbf{r}})\, \mathrm{d}\Omega = \frac{\delta_{mm'}\delta_{nn'}}{(\gamma_{mn})^2}. \tag{49}$$

References

[1] Grandy WT. Scattering of waves from large spheres. Cambridge UK: Cambridge University Press; 2000. p. 70–1.
[2] Bohren CF, Huffman DR. Absorption and scattering of light by small particles. New York: Wiley; 1983 [Section 4].
[3] Videen G, Sun W. Yet another look at light scattering from particles in absorbing media. Appl Opt 2003;42:6724–7.
[4] Fu Q, Sun W. Mie theory for light scattering by a spherical particle in an absorbing medium. Appl Opt 2001;40:1354–61.
[5] Mishchenko MI. Multiple scattering by particles embedded in an absorbing medium. 2. Radiative transfer equation. JQRST 2008;109:2386–90.
[6] Mishchenko MI, Travis LD, Lacis AA. Scattering, absorption, and emission of light by small particles. Cambridge, UK: Cambridge University Press; 2002 [Section 5.1]. Freely available at: ⟨http://www.giss.nasa.gov/~crmim/books.html⟩.
[7] Doicu A, Wriedt T, Eremin YA. Light scattering by systems of particles. Berlin: Springer; 2006 [Appendix D].
[8] Stratton JA. Electromagnetic theory. New York: McGraw-Hill; 1941 [Section 2.19].
[9] Berg MJ, Sorensen CM, Chakrabarti A. Extinction and the optical theorem. Part I. Single particles. J Opt Soc Am A 2008;25:1504–13.
[10] Berg MJ, Sorensen CM, Chakrabarti A. Extinction and the optical theorem. Part II. Multiple particles. J Opt Soc Am A 2008;25:1514–20.
[11] Mishchenko MI. The electromagnetic optical theorem revisited. JQRST 2006;101:404–10.
[12] Mishchenko MI. Far-field approximation in electromagnetic scattering. JQSRT 2006;100:268–76.
[13] Jackson JD. Classical electrodynamics. New York: Wiley; 1999. p. 427.
[14] Abramowitz M, Stegun IA. Handbook of mathematical functions with formulas, graphs, and mathematical tables, 9th ed. Washington, DC: National Bureau of Standards; 1970. p. 437.
[15] Videen G, Pinnick RG, Ngo D, Fu Q, Chýlek P. Asymmetry parameter and aggregate particles. Appl Opt 1998;37:1104–9.
[16] van de Hulst HC. Light scattering by small particles. New York: Dover; 1981 [Section 8.22].
[17] Brillouin L. The scattering cross section of spheres for electromagnetic waves. J Appl Phys 1949;20:1110–25.